Applied Surface Science 292 (2014) 710–716

Contents lists available at ScienceDirect

Applied Surface Science

journal homepage: www.elsevier.com/locate/apsusc

Cd(II) removal from aqueous solution by adsorption on α-ketoglutaric acid-modified magnetic chitosan

Guide Yang[a,b], Lin Tang[a,b,*], Xiaoxia Lei[a,b], Guangming Zeng[a,b], Ye Cai[a,b], Xue Wei[a,b], Yaoyu Zhou[a,b], Sisi Li[a,b], Yan Fang[a,b], Yi Zhang[a,b]

[a] College of Environmental Science and Engineering, Hunan University, Changsha 410082, PR China
[b] Key Laboratory of Environmental Biology and Pollution Control, Hunan University, Ministry of Education, Changsha 410082, Hunan, PR China

ARTICLE INFO

Article history:
Received 24 October 2013
Received in revised form 3 December 2013
Accepted 6 December 2013
Available online 16 December 2013

Keywords:
Chitosan
α-Ketoglutaric acid
Cd(II)
Adsorption
Magnetic separation

ABSTRACT

The present study developed an α-ketoglutaric acid-modified magnetic chitosan (α-KA-Fe_3O_4/CS) for highly efficient adsorption of Cd(II) from aqueous solution. Several techniques, including transmission electron microscopy (TEM), Fourier transform infrared (FTIR) and vibrating sample magnetometer (VSM), were applied to characterize the adsorbent. Batch tests were conducted to investigate the Cd(II) adsorption performance of α-KA-Fe_3O_4/CS. The maximum adsorption efficiency of Cd(II) appeared at pH 6.0 with the value of 93%. The adsorption amount was large and even reached 201.2 mg/g with the initial Cd(II) concentration of 1000 mg/L. The adsorption equilibrium was reached within 30 min and commendably described by pseudo-second-order model, and Langmuir model fitted the adsorption isotherm better. Furthermore, thermodynamic parameters, free energy (ΔG), enthalpy (ΔH) and entropy (ΔS) of Cd(II) adsorption were also calculated and showed that the overall adsorption process was endothermic and spontaneous in nature because of positive ΔH values and negative ΔG values, respectively. Moreover, the Cd(II)-loaded α-KA-Fe_3O_4/CS could be regenerated by 0.02 mol/L NaOH solution, and the cadmium removal capacity could still be kept around 89% in the sixth cycle. All the results indicated that α-KA-Fe_3O_4/CS was a promising adsorbent in environment pollution cleanup.

1. Introduction

Cadmium ion (Cd(II)) is a toxic heavy metal ion, normally found in industrial wastewater, especially in electroplating, smelting, alloy, pigment, and plastic manufacturing, mining, metallurgy and refining [1,2]. Due to its difficult detoxification, cadmium (Cd) has access to be assimilated, gathered and stored by organisms, and eventually, it will be transferred to humans via the food chain, causing serious damage to kidney and bones [3]. US Environment Protection Agency has classified cadmium as group B1 carcinogen, and the world-shaking itai-itai disease event in Toyama Prefecture is caused by prolonged oral Cd ingestion [4]. Therefore, it is indispensable to develop efficient methods for the removal of cadmium from contaminated water.

Adsorption is a relatively promising method among numerous wastewater treatment techniques because of its convenient operation, high efficiency, low cost and easy regeneration [5–8]. It mainly exploits the specific surface structure and pores to immobile pollutants onto the surface of adsorbent in order to achieve the goal of pollutants removal. Several adsorbents, such as activated carbon, biomass, waste materials (including industrial wastes and agricultural wastes), nano-materials (such as carbon nanotube and nano-scale iron) and polymers have been applied to treat contaminated water [9–16] and showed good results. However, these adsorbents are often limited due to the low adsorption capacity, long treating period and easy aggregation. Chitosan, a natural macromolecular substance, because of its widely availability, nontoxicity, biocompatibility and high chelation capacity and chemical activity, shows the superiority in application in electrochemical sensing, carrier, catalysis, as well as absorption [17,18]. Because the autologous amino and two hydroxyl groups which are conducive to chelating and surface contact with pollutants, chitosan has been widely applied as an effective adsorbent for the removal of heavy metals (for example, Cd(II) ions) and organic pollutants from effluent. But the amino groups of chitosan can be easy to transform into quaternary ammonium cations and dissolved in the acidic matrix because of the exchange interaction between with weak basic anions, which may lead to a decrease in the adsorption rate and adsorption amount for Cd(II) removal. Previous study [19] demonstrates that the adsorption behavior of chitosan could be improved by modification towards chitosan

* Corresponding authors at: College of Environmental Science and Engineering, Hunan University, Changsha 410082, PR China. Tel.: +86 731 88822778; fax: +86 731 88822778.
E-mail addresses: yang89_0811@126.com (G. Yang), tanglin@hnu.edu.cn, iluenjor@hnu.edu.cn (L. Tang), zgming@hnu.edu.cn (G. Zeng).

0169-4332/$ – see front matter © 2013 Elsevier B.V. All rights reserved.
http://dx.doi.org/10.1016/j.apsusc.2013.12.038

surface, which includes the addition of functional groups [20] and magnetic nanoparticles [21]. Thus, the stability and application scope of chitosan can be markedly enhanced.

Magnetic composite particles, for example, Fe_3O_4 nanoparticles, have been successfully applied in magnetic separation and detoxification or recovery of pollutants [22,23]. The magnetism modification of the surface of target supports can be convenient and effective for solid-liquid separation and the regeneration of adsorbents in the removal of pollutants from wastewater. At the same time, the functionalization of chitosan with α-ketoglutaric acid can introduce carbonyl and keto groups, which can chelate with heavy metal ions through electrostatic interaction, boosting the removal of target pollutants [24,25].

Herein, the objectives of this study were to synthesize an α-ketoglutaric acid modified chitosan combined with magnetic Fe_3O_4 nanoparticle (α-KA-Fe_3O_4/CS) through a simple co-condensation method and following redox process, to characterize the composite using a variety of physicochemical techniques, and to evaluate the Cd(II) adsorption performance of resultant samples. Some factors affecting the adsorption of Cd(II), such as pH, initial concentration, contact time and temperature were investigated. The relevant removal mechanisms of Cd(II) onto α-KA-Fe_3O_4/CS were well expounded via adsorption kinetics, isotherms and thermodynamics. Regeneration and reusability were also examined for further application of this new type of adsorbent to more complex water environment.

2. Materials and methods

2.1. Preparation of magnetic chitosan

Fe_3O_4 magnetic nanoparticles were first synthesized by conventional chemical coprecipitation method [26]. Briefly, $FeCl_3{\cdot}6H_2O$ and $FeCl_2{\cdot}4H_2O$ with the molar ratio of 3:2 (superfluous $FeCl_2{\cdot}4H_2O$ to prevent the oxidation of Fe_3O_4 nanoparticles) were dissolved in N_2 gas bubbled ultrapure water. Then, a certain amount of 4 mol/L ammonia solution was added rapidly under vigorous mechanical stirring to adjust the solution pH to ~10.0. The reaction was maintained for 30 min at 70 °C. The resultant nanoparticles were separated using high density magnet, followed by repeated washing with ultrapure water to neutrality. Finally, they were vacuum-desiccated at 70 °C and then stored in a nitrogen-filled glovebox until required.

Then, the magnetic chitosan composites (Fe_3O_4/CS) were prepared through a co-casting method. Typically, the chitosan solution was prepared by melting 0.225 g chitosan into 150 mL acetic acid (1%). Then, the certain amount of Fe_3O_4 nanoparticles (0.1125 g) were added into 150 mL ultrapure water and ultrasonicated for 30 min to obtain slurry. Follow on it, the above chitosan solution was dropped into the dispersed Fe_3O_4 slurry under stirring. Furthermore, 60 mL sodium polyphosphate solution (1%) was added dropwise. After continuing stirring for 8 h, the solid was separated by magnet. The obtained product was washed several times with absolute ethanol and ultrapure water until pH was neutral, vacuum freeze-dried for 24 h and stored for further experiments.

2.2. Magnetic chitosan modified with α-ketoglutaric acid

Magnetic chitosan was modified with α-ketoglutaric acid according to the method described previously with some modifications [25]. Typically, 0.25 g α-ketoglutaric acid was dissolved into 50 mL acetic acid buffer solution containing 100 mg magnetic chitosan (pH 5.6). Then, the mixture was adjusted by 0.1 mol/L NaOH solution to ~5.0 of pH under stirring, and a small quantity of sodium borohydride (molar ratio of sodium borohydride and α-ketoglutaric acid was 1.8:1) was added slowly, and continuing, the mixed solution pH was adjusted to ~7.0 by 0.1 mol/L HCl. After stirring for 24 h, the obtained solid was separated by magnet, and washed 3–4 times with ethanol and diethyl ether, vacuum freeze-dried for 24 h to obtain the expectant adsorbent (α-KA-Fe_3O_4/CS).

2.3. Characterization of adsorbent

Transmission electron microscopy (TEM) images were performed on a JEOL-1230 Electron Microscope operated at 100 kV. Fourier transform infrared (FTIR) spectra of the materials were recorded on a Nicolet NEXUS 670 FT-IR Spectrometer by the standard KBr disk method. The magnetic properties of the samples were studied by a vibrating sample magnetometer (VSM) at room temperature.

2.4. Preparation of cadmium solutions

Stock solution of Cd(II) ions with a concentration of 1000 mg/L was prepared by dissolving $Cd(NO_3)_2{\cdot}4H_2O$ (analytical reagent grade) in ultrapure water. The desired Cd(II) concentrations were prepared from the stock solution by diluting for each adsorption experiment.

2.5. Batch adsorption experiments

Adsorption experiments were carried out by mixing 0.04 g α-KA-Fe_3O_4/CS with 30 mL of solution of varying cadmium concentrations at 25 ± 1 °C. Batch tests were carried out in 100 mL of polyethylene terephthalate (PET) bottles at 150 rpm for 90 min unless otherwise noted. The pH of the solution was adjusted by adding either 0.1 mol/L NaOH or 0.1 mol/L HNO_3. After finishing adsorption, the adsorbent was magnetically separated and the supernatant was collected for Cd(II) measurement. All experiments were performed in duplicate with the averaged values reported here. Cadmium concentration was determined by atomic absorption spectroscopy (AAS Hitachi Z-8100, Japan).

The quantity of cadmium adsorbed at equilibrium and time t was calculated by the following expression:

$$q_e = \frac{(c_0 - c_e)V}{1000m} \quad (1)$$

$$q_t = \frac{(c_0 - c_t)V}{1000m} \quad (2)$$

where m was the mass of adsorbent (g), V was the volume of the solution (mL), c_0 was the initial concentration of cadmium (mg/L), c_e and c_t were the cadmium concentration (mg/L) at equilibrium and time t, respectively, and q_e and q_t were the amount of cadmium adsorbed per unit mass of adsorbent (mg/g) at equilibrium and time t, respectively.

For the calculation of the cadmium adsorption rate (R), the following expression was used:

$$R = \frac{c_0 - c_e}{c_0} \times 100\% \quad (3)$$

where c_0 and c_e was the cadmium initial and equilibrium concentrations (mg/L) in the solution, respectively.

2.6. Regeneration and reuse of α-KA-Fe_3O_4/CS

Regeneration and reusability are very important for the practical application of the adsorption method. In this study, experiments related to the regeneration of α-KA-Fe_3O_4/CS and Cd(II) re-adsorption were carried out in six consecutively adsorption/desorption cycles. For each cycle, 30 mL of 100 mg/L Cd(II)

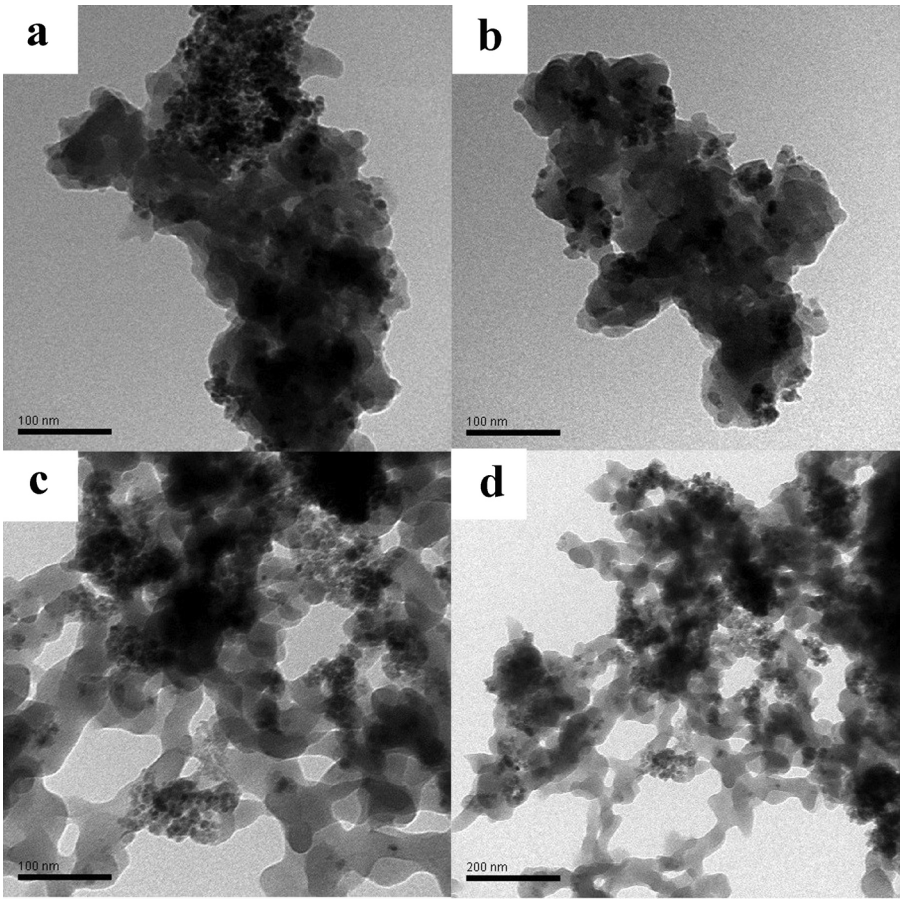

Fig. 1. TEM images of Fe_3O_4/CS (a, b) and α-KA-Fe_3O_4/CS (c, d).

solution was adsorbed first by 0.04 g of adsorbent for 90 min to reach adsorption equilibrium. The supernatant was decanted with an assistance of the permanent magnet and the Cd(II)-loaded adsorbent was then desorbed with 40 mL of 0.02 mol/L NaOH solution for 120 min. After each cycle of adsorption/desorption, α-KA-Fe_3O_4/CS was washed thoroughly with ultrapure water to neutrality and then reconditioned for adsorption in the succeeding cycle.

3. Results and discussion

3.1. Characterization

Fig. 1 showed TEM images of Fe_3O_4/CS and α-KA-Fe_3O_4/CS. It was observed that the aggregation of Fe_3O_4/CS nanoparticles emerged seriously. However, after modifying with α-ketoglutarate acid, there occurred many entangled network of structures, thus enlarging the effective contact area with heavy metals. Simultaneously, the introduction of α-ketoglutarate acid made magnetic nanoparticles more uniformly distributed in α-KA-Fe_3O_4/CS than it in pristine Fe_3O_4/CS, which indicated that the dispersity was improved after modifying with α-ketoglutarate acid. The FTIR spectra of Fe_3O_4 (a), Fe_3O_4/CS (b) and α-KA-Fe_3O_4/CS (c) was shown in Fig. 2a, The peaks at 570 cm^{-1} aiming at Fe_3O_4 spectrum, belonged to Fe-O stretching vibration [27], which also occurred in the Fe_3O_4/CS spectrum and α-KA-Fe_3O_4/CS spectrum, implying that the Fe_3O_4 nanoparticles were successful prepared and introduced into the chitosan. In the spectrum of Fe_3O_4/CS, the strong peaks at 2923 and 2853 cm^{-1} belonged to the C-H stretching vibration of the polymer backbone, and the band at around 1073 and 1487 cm^{-1} were contributed to the C—O and chitosan ring stretching vibration peak, respectively [20]. Moreover, in a comparison of the two FTIR spectra of Fe_3O_4/CS and α-KA-Fe_3O_4/CS, it could be clearly seen that the chemical modification significantly altered the FTIR pattern of Fe_3O_4/CS. The characteristic absorption band around 1620 cm^{-1} attributed to the vibration of N—H in amine (—NH_2), occurring in the curve of α-KA-Fe_3O_4/CS, and the absorption bands at 1718 cm^{-1} and 1402 cm^{-1} could be observed in the pattern of α-KA-Fe_3O_4/CS, but not present in the pattern of Fe_3O_4/CS. The absorbance band at 1402 cm^{-1} was the C—H stretch vibration from R—CH_2—COOH, and the absorbance band at 1718 cm^{-1} showed the presence of the carbonyl groups. The peaks at 3455 cm^{-1} of the three spectra were contributed to the H—O—H, derived from crystal water adsorbed onto the surface of the three particles. The saturated magnetization of Fe_3O_4/CS (a) and α-KA-Fe_3O_4/CS (b) were 26.42 emu/g and 20.26 emu/g, respectively (shown in Fig. 2b). The decrease might be due to the existence of large amounts of net structures after modifying with α-ketoglutaric acid, strengthening the sinking resistance of adsorbent in the solution, but it was still easily attracted by high density magnet and separated from liquid phase [28].

3.2. Effect of solution pH

The solution pH significantly influences the surface properties and the protonation degree of adsorbent [29]. Considering that the precipitation of cadmium hydroxide would be likely to form at high pH value, in this study, pH values above 8 was not applied. Removal efficiency of Cd(II) on the resultant composites as a function of solution pH with an initial Cd(II) concentration of 100 mg/L were shown in Fig. 3a. It exhibited that the Cd(II) adsorption capacity got obviously improved on the whole after modifying with α-ketoglutaric

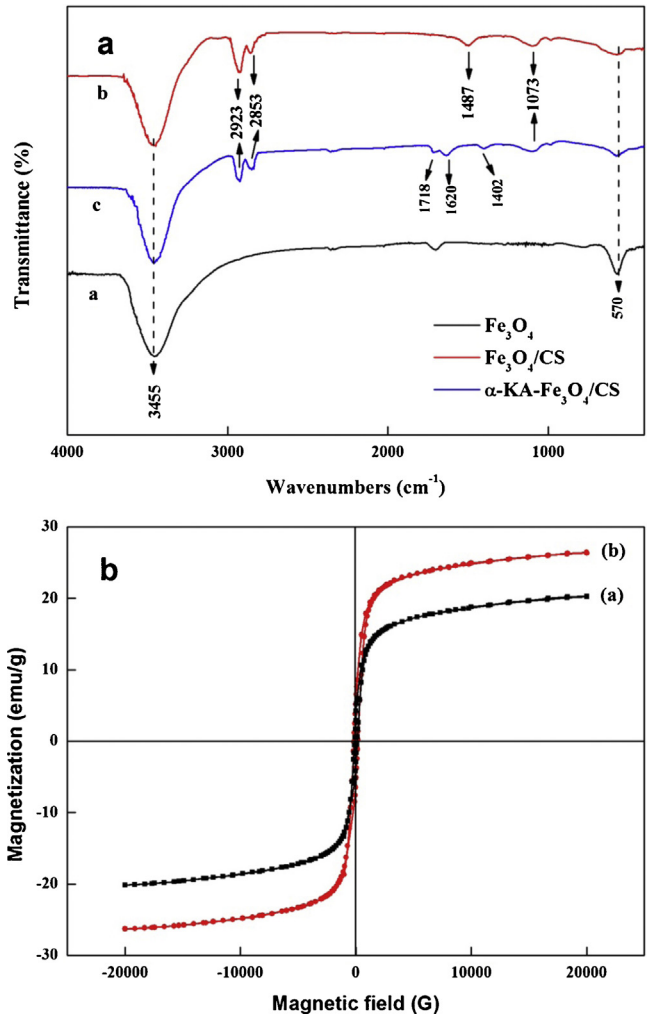

Fig. 2. (a) FTIR spectra of Fe_3O_4, Fe_3O_4/CS and α-KA-Fe_3O_4/CS and (b) magnetization curves of Fe_3O_4/CS and α-KA-Fe_3O_4/CS.

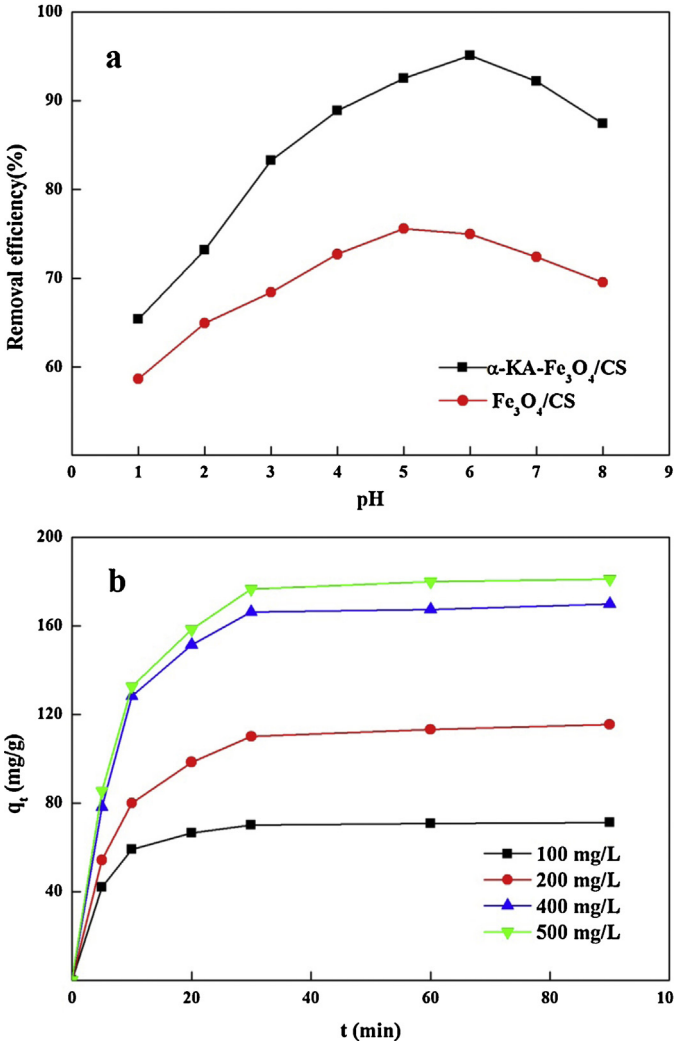

Fig. 3. (a) Effect of pH on removal of Cd(II) (Initial Cd(II) concentration: 100 mg/L, adsorbent dose: 0.04 g, contact time: 90 min and temperature: 25 °C) and (b) effect of contact time and initial concentration on removal of different initial concentrations Cd(II) (adsorbent dose: 0.04 g, pH value: 6.0 and temperature: 25 °C).

acid. The improvement was related with the net structures of α-KA-Fe_3O_4/CS, which accelerated the contact between the adsorbent with Cd(II). The solution pH significantly affected the adsorption capacity of α-KA-Fe_3O_4/CS, and the adsorption efficiency reached the maximum values of 93% when the solution pH was 6.0, and it decreased by either increasing or lowering pH under the present range of the experimental condition. The similar trends have been reported by many studies that the adsorption of Cd(II) onto adsorbent was low at strongly acidic pH while increasing at higher pH values [30–32]. This adsorption behavior also could be explained by surface charge and proton-competitive adsorption. At lower pH values, the charge on the surface of α-KA-Fe_3O_4/CS was positive [33], and thus, a significant electrostatic repulsion existed between the positively charged surface and the cationic Cd(II) ions, which inhibited the adsorption of Cd(II). At the same time, in this acidic medium, the Cd(II) ions adsorption onto the adsorbent was limited related with H^+ ions, which competed with the Cd(II) ions for the available adsorption sites. Contrarily, with the solution pH increase, the number of positively charged sites decreased and the number of negatively charged sites increased on the surface of adsorbents. Obviously, a negatively charged surface site did favor the adsorption of cationic Cd(II) ions because of electrostatic attraction. On the other hand, the Cd(II) ions were prone to $Cd(OH)_2$ deposition through hydrolysis at higher solution pH values, and the aggregation effect between Cd(II) with OH^- also led to the decreasing of removal efficiency [34].

3.3. *Effect of contact time and initial Cd(II) concentration*

Fig. 3b depicted the Cd(II) adsorption as a function of contact time with different initial Cd(II) concentrations (from 100 to 500 mg/L) at solution pH 6.0. The adsorption rate was quite fast, an initial fast step was completed within 10 min, with that followed by a slower second stage, and finally, adsorption equilibrium was achieved within 30 min. Contact time had no significant effect on Cd(II) adsorption at different initial Cd(II) concentrations, demonstrating a very strong bonding force existed between α-KA-Fe_3O_4/CS and Cd(II). The fast adsorption rate might be connected with the introduction of Fe_3O_4 nanoparticles and α-ketoglutaric acid. At the same time, the micro-nano net structure of adsorbent could expand the effective contact area with Cd(II), and the generated carbonyl group, imino group and carboxyl group also could accelerate the removal of the target pollutant by electrostatic interaction and chelation. The Cd(II) adsorption also showed an admirable result, and it could reach 181.2 mg/g when the initial Cd(II) concentration was 500 mg/L, which embodied the advantage of α-KA-Fe_3O_4/CS to remove cadmium ion in aqueous solution. It

Table 1
Adsorption kinetic model parameters for Cd(II) adsorption on α-KA-Fe_3O_4/CS at different Cd(II) initial concentrations.

Initial concentration (mg/L)	Pseudo-first-order model			Pseudo-second-order model		
	K_1 (min^{-1})	$q_{e,exp}$ (mg/g)	R_1^2	K_2 (g/mg/min)	$q_{e,cal}$ (mg/g)	R_2^2
100	0.367	71.33	0.939	0.0053	73.64	0.999
200	0.257	116.5	0.923	0.0016	122.85	0.999
400	0.287	174.6	0.704	0.0013	179.21	0.998
500	0.294	186.8	0.734	0.0012	191.94	0.998

was not difficult to find that the difference of adsorption capacity was dwindled with the homogeneous increasing of the initial Cd(II) concentration, indicating the adsorption gradually reached saturation at high initial Cd(II) concentration, and available adsorption sites between adsorbent and Cd(II) was on the decline.

3.4. Adsorption kinetics

Kinetics of adsorption is an important characteristic in defining the efficiency of adsorption [30]. Two common kinetic models, pseudo-first-order and pseudo-second-order kinetic models were applied to fit the Cd(II) adsorption kinetic data to get an insight of the adsorption rate of Cd(II) onto α-KA-Fe_3O_4/CS and to determine the rate-limiting step of the transport mechanism [35].

The relevant equations Eq. (4) (pseudo-first-order model) and Eq. (5) (pseudo-second-order model) are as follows:

$$\ln(q_e - q_t) = \ln q_e - k_1 t \tag{4}$$

$$\frac{t}{q_t} = \frac{1}{k_2 q_e^2} + \frac{t}{q_e} \tag{5}$$

where q_e and q_t (mg/g) was the amount of removed Cr(VI) at equilibrium and at time t, respectively, k_1 (min^{-1}) and k_2 (g/mg/min) was the pseudo-first-order rate constant and pseudo-second-order rate constant, respectively.

Aim at the pseudo-first-order kinetic model, the values of k_1 and q_e were calculated from the slope and intercept of the linear plot of $\ln(q_e - q_t)$ versus t at different initial Cd(II) concentrations (Fig. 4a). The values of correlation coefficient (R^2) and rate constants at various concentrations of Cd(II) are given in Table 1. It could be found that the q_e values obtained were 71.33, 116.5, 174.6 and 186.8 mg/g with the initial Cd(II) concentrations of 100, 200, 400 and 500 mg/L, respectively. The results were different from the experimental q_e values, and the correlation coefficients were lower compared with that of pseudo-second-order kinetic model. The above results indicated that the adsorption process could not be well fitted with pseudo-first-order kinetic model.

On the other hand, the pseudo-second-order kinetic model could match well the experimental data (shown in Fig. 4b) with high correlation coefficients ($R^2 > 0.99$) (Table 1). The values of q_e calculated from the pseudo-second-order kinetic models were in good agreement with those obtained from experiment. This confirmed that the adsorption process was dominated by chemical reaction involving valence forces through sharing or exchanging of electrons [36].

3.5. Adsorption isotherms

In ordered to make clear the detailed Cd(II) adsorption process, the adsorption isotherms of α-KA-Fe_3O_4/CS are evaluated by changing the initial concentration of Cd(II) from 10 to 1000 mg/L. The Cd(II) removal capacity increase with the initial Cd(II) concentration increase, and the maximum Cd(II) adsorption capacity even reached 201.2 mg/g with the initial Cd(II) concentration of 1000 mg/L, which was relative high compared with previous study [32,9]. The calculated parameters based on Langmuir adsorption

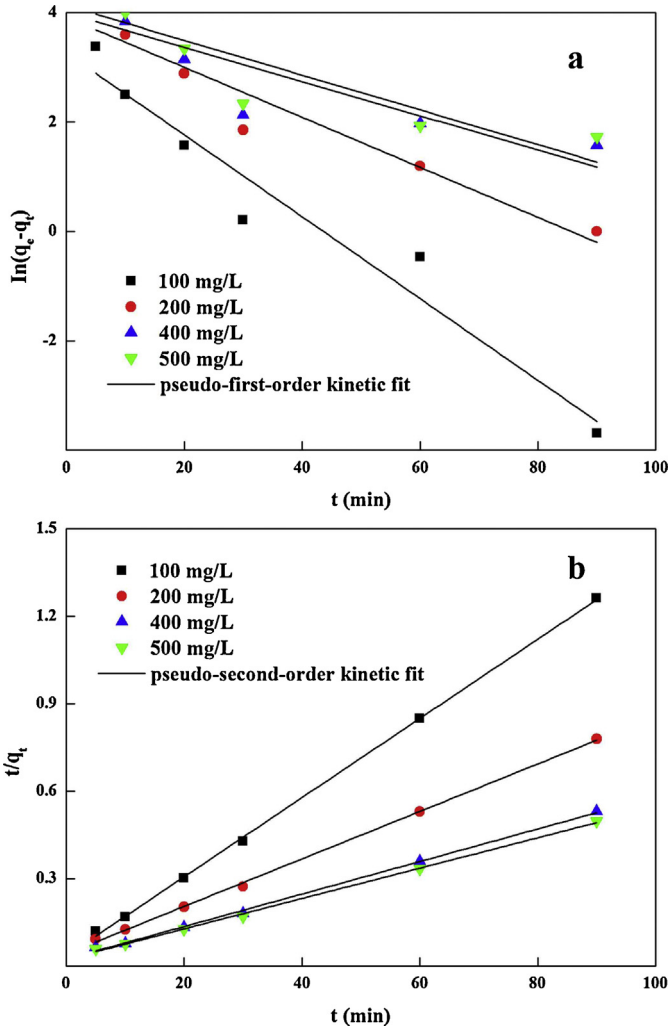

Fig. 4. Linear fit of experimental data using pseudo-first-order kinetic (a) and pseudo-second-order kinetic (b) model.

model and Freundlich adsorption model were listed in Table 2. Langmuir and Freundlich adsorption isotherm models, which assumed that the adsorption occurs on homogeneous surface sites and heterogeneous surface sites, respectively, could be expressed as

$$\text{Langmuir}: \ q_e = \frac{q_m K_L c_e}{1 + K_L c_e} \tag{6}$$

Table 2
Adsorption parameters for the Langmuir and Freundlich isotherm models (adsorbent dose: 0.04 g, pH value: 6.0, contact time: 90 min and temperature: 25 °C).

Langmuir			Freundlich		
K_L (L/mg)	q_m (mg/g)	R_1^2	K_F	n	R_2^2
0.0042	255.77	0.993	9.235	2.189	0.931

$$\text{Freundlich}: q_e = K_F c_e^{1/n} \quad (7)$$

where q_e (mg/g) was the amount of Cd(II) adsorbed at equilibrium, q_m (mg/g) was the maximum adsorption capacity, c_e (mg/L) was the equilibrium solute concentration, K_L (L/mg) was the Langmuir constant related to adsorption energy, K_F and n were Freundlich constants and intensity factors, respectively.

It could come to conclusion that the Langmuir model could better describe the adsorption result of Cd(II) with the higher correlation coefficient R^2 ($R^2 > 0.99$), indicating that the adsorbed cadmium ions formed monolayer coverage on the adsorbent surface and all adsorption sites were equal with uniform adsorption energies without any interaction between the adsorbed molecules. Similar results had also been observed by other adsorbents, such as poly(methacrylic acid)-grafted chitosan [20], natural and modified rice husk [32] and alumina [37]. The dimensionless constant (R_L) called separation factor or equilibrium parameter was given according to Eq. (8).

$$R_L = \frac{1}{1 + K_L c_0} \quad (8)$$

where c_0 (mg/L) is the initial Cu (II) concentration, K_L (L/mg) was the Langmuir constant.

It wasn't difficult to find that all the R_L values were between 0 and 1 due to the positive values of K_L, indicating that the adsorption of Cd(II) on α-KA-Fe_3O_4/CS was favorable. Moreover, the R_L values decreased as the initial Cd(II) concentration increased, suggesting that the adsorption process was more favorable at higher initial Cd(II) concentrations, which was also proved by the intensity factor of Freundlich model since $n > 1$, implying that adsorption intensity was favorable at high concentrations and much less at lower concentrations.

3.6. Adsorption thermodynamics

The Cd(II) adsorption process was evaluated at different temperatures between 25 °C and 75 °C. Thermodynamic parameters such as free energy change (ΔG), enthalpy change (ΔH) and entropy change (ΔS) were calculated by using the following well known thermodynamics equations (9)–(11):

$$K_b = \frac{q_e}{c_e} \quad (9)$$

$$\ln K_b = \frac{\Delta S}{R} - \frac{\Delta H}{RT} \quad (10)$$

$$\Delta G = \Delta H - T\Delta S \quad (11)$$

where K_b was the equilibrium constant, q_e and c_e were Cd(II) equilibrium adsorption capacity (mg/g) and equilibrium concentrations (mg/L) of α-KA-Fe_3O_4/CS, respectively. R was the gas constant (8.314 J/mol/K), T was the absolute temperature (K), and ΔS (J/mol/K), ΔH (kJ/mol) and ΔG (kJ/mol) were the changes in the entropy, enthalpy and Gibb's free energy of the system, respectively.

The values of ΔH and ΔS were calculated from the slope and intercept of Von't Hoff plot of log K_b versus $1/T$ and their values were recorded in Table 3. The ΔH of Cd(II) adsorption on α-KA-Fe_3O_4/CS was 10.21 kJ/mol, indicating that the adsorption of Cd(II) was an endothermic process. The positive ΔS value ($\Delta S = 58.92$ J/mol/K) demonstrated the increased randomness at the solid–liquid interface during the adsorption of Cd(II). The ΔG of Cd(II) adsorption processes were all negative, illustrating that the adsorption processes were thermodynamically feasible and spontaneous at the studied temperatures [38].

Table 3
Thermodynamic parameters for Cd(II) adsorption on α-KA-Fe_3O_4/CS (Initial Cd(II) concentration: 100 mg/L, adsorbent dose: 0.04 g, pH value: 6.0 and contact time: 90 min).

Temperature (°C)	K_b (L/g)	ΔS (J/K/mol)	ΔH (kJ/mol)	ΔG (kJ/mol)
25	19.41			−7.36
35	21.22			−7.65
45	25.32	58.92	10.21	−8.54
60	30.25			−9.42
75	35.36			−10.3

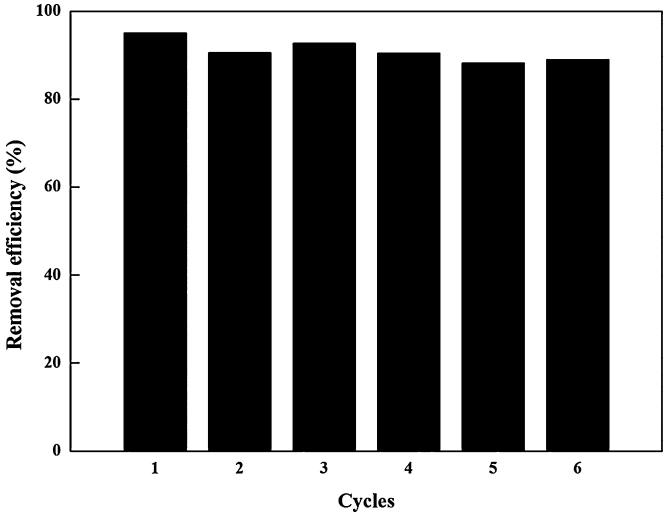

Fig. 5. Six consecutive adsorption-desorption cycles of α-KA-Fe_3O_4/CS for Cd(II) (initial Cd(II) concentration: 100 mg/L, adsorbent dose: 0.04 g, pH value: 6.0, contact time: 90 min, temperature: 25 °C, desorption agent: 40 mL of 0.02 mol/L NaOH and desorption time: 120 min).

3.7. Regeneration and reuse of α-KA-Fe_3O_4/CS

Regeneration of the adsorbent for reutilization is of crucial importance in industrial practice for heavy metals removal from wastewater [39]. In this study, desorption and re-adsorption tests were conducted to investigate the regeneration performance of α-KA-Fe_3O_4/CS using 0.02 mol/L NaOH solutions for the desorption of Cd(II) and the result was shown in Fig. 5. The regenerated α-KA-Fe_3O_4/CS adsorbent could still keep approximately 89% of its cadmium ions removal capacity in the sixth consecutive adsorption-regeneration cycle, indicating that the regeneration of α-KA-Fe_3O_4/CS by NaOH solution was quite effective and this adsorbent had potential application value in industrial-scale practice.

4. Conclusions

The aim of this study was to prepare an α-ketoglutaric acid-modified magnetic chitosan for effectively removing Cd(II) from aqueous solution. TEM and FTIR analyses indicated Fe_3O_4 nanoparticles and α-ketoglutaric acid were successfully loaded onto the chitosan, and VSM measurement revealed that the nano-adsorbent had very good magnetic property with the saturated magnetization of 20.26 emu/g. The Cd(II) adsorption experiments indicated that α-KA-Fe_3O_4/CS was a promising adsorbent and showed very good result for the adsorption of Cd(II). The adsorption efficiency was dependent on pH and the rate was also very fast, only 30 min was needed to reach adsorption equilibrium. Equilibrium adsorption data was commendably fitted by pseudo-second-order kinetic model and the adsorption process was described well by the Langmuir model. Thermodynamic studies demonstrated that the

adsorption process took place spontaneously with a negative free energy change. The adsorbent could be used repeatedly by effective regeneration using 0.02 mol/L NaOH solution and the adsorption efficiency still reached around 89% after six consecutive adsorption-regeneration cycles. The above results indicate that α-KA-Fe_3O_4/CS, with excellent Cd(II) adsorption capacity and strong regeneration capacity, shows great potential in the application of wastewater treatment.

Acknowledgements

The study was financially supported by Program for the Outstanding Young Talents of China, the National Natural Science Foundation of China (51222805), the Program for New Century Excellent Talents in University from the Ministry of Education of China (NCET-11-0129), Interdisciplinary Research Project of Hunan University, China Scholarship Council (CSC) (2010843195), the Fundamental Research Funds for the Central Universities, Hunan University, and Foundation for the Author of Excellent Doctoral Dissertation of Hunan Province.

References

[1] V.K. Gupta, A. Rastogi, Equilibrium and kinetic modelling of cadmium(II) biosorption by nonliving algal biomass *Oedogonium* sp. from aqueous phase, J. Hazard. Mater. 153 (2008) 759–766.
[2] Y. Ding, D.B. Jing, H.L. Gong, L.B. Zhou, X.S. Yang, Biosorption of aquatic cadmium(II) by unmodified rice straw, Bioresour. Technol. 114 (2012) 20–25.
[3] R.R. Leyva, J.R. Mendez, J.B. Mendoza, L.F. Rubio, R.M. Guerrero, Adsorption of cadmium(II) from aqueous solution onto activated carbon, Water Sci. Technol. 35 (1997) 205–210.
[4] T. Inabaa, E. Kobayashi, Y. Suwazono, M. Uetani, M. Oishi, H. Nakagawa, K. Nogawa, Estimation of cumulative cadmium intake causing Itai-itai disease, Toxicol. Lett. 2 (2005) 192–201.
[5] A. Mittal, V.K. Gupta, A. Malviya, J. Mittal, Process development for the batch and bulk removal and recovery of a hazardous, water-soluble azo dye (Metanil Yellow) by adsorption over waste materials (Bottom Ash and De-Oiled Soya), J. Hazard. Mater. 151 (2008) 821–832.
[6] M. Machida, B. Fotoohi, Y. Amamo, L. Mercier, Cadmium(II) and lead(II) adsorption onto hetero-atom functional mesoporous silica and activated carbon, Appl. Surf. Sci. 258 (2012) 7389–7394.
[7] A. Mittal, L. Kurup (Krishnan), V.K. Gupta, Use of waste materials-Bottom Ash and De-Oiled Soya, as potential adsorbents for the removal of Amaranth from aqueous solutions, J. Hazard. Mater. 117 (2005) 171–178.
[8] A. Mittal, J. Mittal, A. Malviya, D. Kaur, V.K. Gupta, Adsorption of hazardous dye crystal violet from wastewater by waste materials, J. Colloid Interface Sci. 343 (2010) 463–473.
[9] A.F. Tajar, T. Kaghazchi, M. Soleimani, Adsorption of cadmium from aqueous solutions on sulfurized activated carbon prepared from nut shells, J. Hazard. Mater. 165 (2009) 1159–1164.
[10] V.K. Gupta, A. Rastogi, A. Nayak, Biosorption of nickel onto treated alga (*Oedogonium hatei*): application of isotherm and kinetic models, J. Colloid Interface Sci. 342 (2010) 533–539.
[11] V.K. Gupta, A. Mittal, L. Krishnan, J. Mittal, Adsorption treatment and recovery of the hazardous dye, Brilliant Blue FCF, over bottom ash and de-oiled soya, J. Colloid Interface Sci. 293 (2006) 16–26.
[12] V.K. Gupta, A. Mittal, L. Kurup, J. Mittal, Adsorption of a hazardous dye, erythrosine, over hen feathers, J. Colloid Interface Sci. 304 (2006) 52–57.
[13] V.K. Gupta, R. Jain, S. Varshney, Removal of Reactofix golden yellow 3 RFN from aqueous solution using wheat husk-An agricultural waste, J. Hazard. Mater. 142 (2007) 443–448.
[14] V.K. Gupta, S. Agarwal, T.A. Saleh, Chromium removal by combining the magnetic properties of iron oxide with adsorption properties of carbon nanotubes, Water Res. 45 (2011) 2207–2212.
[15] H.K. Boparai, M. Joseph, D.M. O'Carroll, Kinetics and thermodynamics of cadmium ion removal by adsorption onto nano zerovalent iron particles, J. Hazard. Mater. 186 (2011) 458–465.
[16] W.M. Yang, L.K. Liu, W. Zhou, W.Z. Xu, Z.P. Zhou, W.H. Huang, Preparation and evaluation of hollow molecular imprinted polymer for adsorption of dibenzothiophene, Appl. Surf. Sci. 258 (2012) 6583–6589.
[17] L. Tang, G.M. Zeng, G.L. Shen, Y.P. Li, Y. Zhang, D.L. Huang, Rapid detection of picloram in agricultural field samples using a disposable immunomembrane-based electrochemical sensor, Environ. Sci. Technol. 42 (2008) 1207–1212.
[18] Y.H. Zhua, J. Hua, J.L. Wang, Competitive adsorption of Pb(II), Cu(II) and Zn(II) onto xanthate-modified magnetic chitosan, J. Hazard. Mater. 221–222 (2012) 155–161.
[19] X.X. Lei, L. Tang, G.M. Zeng, M.S. Wu, Y.Y. Zhou, Y. Pang, Y.Y. Liu, Z. Li, G.D. Yang, Study on magnetic chitosan microparticles for rapid removal of heavy metals, Adv. Mater. Res. 518-523 (2012) 2844–2848.
[20] L.Q. Huang, S.J. Yuan, L. Lv, G.Q. Tan, B. Liang, S.O. Pehkonen, Poly(methacrylic acid)-grafted chitosan microspheres via surfaceinitiated ATRP for enhanced removal of Cd(II) ions from aqueous solution, J. Colloid Interface Sci. 405 (2013) 171–182.
[21] Y.W. Chen, J.L. Wang, Preparation and characterization of magnetic chitosan nanoparticles and its application for Cu(II) removal, Chem. Eng. J. 168 (2011) 286–292.
[22] L. Tang, M.S. Wu, G.M. Zeng, J. Yin, Y.Y. Liu, X.X. Lei, Z. Li, Y. Zhang, J.C. Zhang, X.Z. Yuan, Magnetic separation and detection of a cellulase gene using core-shell nanoparticle probes towards Q-PCR assay, Anal. Methods 4 (2012) 2914–2921.
[23] G.M. Zeng, Y. Pang, Z.T. Zeng, L. Tang, Y. Zhang, Y.Y. Liu, J.C. Zhang, X.X. Lei, Z. Li, Y.Q. Xiong, G.X. Xie, Removal and recovery of Zn^{2+} and Pb^{2+} by imine-functionalized magnetic nanoparticles with tunable selectivity, Langmuir 28 (2012) 468–473.
[24] Y.T. Zhou, C.B. White, H.L. Nie, L.M. Zhu, Adsorption mechanism of Cu^{2+} from aqueous solution by chitosan-coated magnetic nanoparticles modified with α-ketoglutaric acid, Colloids Surf. B 74 (2009) 244–252.
[25] Y.T. Zhou, H.L. Nie, C.B. White, Z.Y. He, L.M. Zhu, Removal of Cu^{2+} from aqueous solution by chitosan-coated magnetic nanoparticles modified with α-ketoglutaric acid, J. Colloid Interface Sci. 330 (2009) 29–37.
[26] Y. Zhang, G.M. Zeng, L. Tang, D.L. Huang, X.Y. Jiang, Y.N. Chen, A hydroquinone biosensor using modified core-shell magnetic nanoparticles supported on carbon paste electrode, Biosens. Bioelectron. 22 (2007) 2121–2126.
[27] Y. Pang, G.M. Zeng, L. Tang, Y. Zhang, Y.Y. Liu, X.X. Lei, Z. Li, J.C. Zhang, G.X. Xie, PEI-grafted magnetic porous powder for highly effective adsorption of heavy metal ions, Desalination 281 (2011) 278–284.
[28] W.W. Tang, G.M. Zeng, J.L. Gong, Y. Liu, X.Y. Wang, Y.Y. Liu, Z.F. Liu, L. Chen, X.R. Zhang, D.Z. Tu, Simultaneous adsorption of atrazine and Cu (II) from wastewater by magnetic multi-walled carbon nanotube, Chem. Eng. J. 211–212 (2012) 470–478.
[29] V.K. Gupta, R. Jain, A. Mittal, M. Mathur, S. Sikarwar, Photochemical degradation of the hazardous dye Safranin-T using TiO_2 catalyst, J. Colloid Interface Sci. 309 (2007) 464–469.
[30] M.S. Mansour, M.E. Ossman, H.A. Farag, Removal of Cd(II) ion from waste water by adsorption onto polyaniline coated on sawdust, Desalination 272 (2011) 301–305.
[31] F.Y. Wang, H. Wang, J.W. Ma, Adsorption of cadmium (II) ions from aqueous solution by a new low-cost adsorbent-Bamboo charcoal, J. Hazard. Mater. 177 (2010) 300–306.
[32] H.P. Ye, Q. Zhu, D.Y. Du, Adsorptive removal of Cd(II) from aqueous solution using natural and modified rice husk, Bioresour. Technol. 101 (2010) 5175–5179.
[33] M. Kumar, B.P. Tripathi, V.K. Shahi, Crosslinked chitosan/polyvinyl alcohol blend beads for removal and recovery of Cd(II) from wastewater, J. Hazard. Mater. 172 (2009) 1041–1048.
[34] F. Gode, E. Pehlivan, A comparative study of two chelating ion-exchange resins for the removal of chromium (III) from aqueous solution, J. Hazard. Mater. B 100 (2003) 231–243.
[35] W.J. Yang, P. Ding, L. Zhou, J.G. Yu, X.Q. Chen, F.P. Jiao, Preparation of diamine modified mesoporous silica on multi-walled carbon nanotubes for the adsorption of heavy metals in aqueous solution, Appl. Surf. Sci. 282 (2013) 38–45.
[36] P. Xu, G.M. Zeng, D.L. Huang, C. Lai, M.H. Zhao, Zh. Wei, N.J. Li, Ch. Huang, G.X. Xie, Adsorption of Pb(II) by iron oxide nanoparticles immobilized *Phanerochaete chrysosporium*: equilibrium, kinetic, thermodynamic and mechanisms analysis, Chem. Eng. J. 203 (2012) 423–431.
[37] Y.J.O. Asencios, M.R.S. Kou, Synthesis of high-surface-area (-Al_2O_3 from aluminum scrap and its use for the adsorption of metals: Pb(II), Cd(II) and Zn(II), Appl. Surf. Sci. 258 (2012) 10002–10011.
[38] J.V.F. Cano, R.L. Ramos, J.M. Barron, R.M.G. Coronado, A.A. Pina, G.J.L. Delgado, Sorption mechanism of Cd(II) from water solution onto chicken eggshell, Appl. Surf. Sci. 276 (2013) 682–690.
[39] V.K. Gupta, Arunima Nayak, Cadmium removal and recovery from aqueous solutions by novel adsorbents prepared from orange peel and Fe_2O_3 nanoparticles, Chem. Eng. J. 180 (2012) 81–90.